The Abdus Salam International Centre for Theoretical Physics

United Nations Educational, Scientific and Cultural Organization

IAEA International Atomic Energy Agency

2267-23

Joint ITER-IAEA-ICTP Advanced Workshop on Fusion and Plasma Physics

3 - 14 October 2011

Dust in tokamaks

DE ANGELIS Umberto

Universita' di Napoli 'Federico II'
Dip. di Scienze Fisiche, Complesso Universitario Monte S. Angelo
via Cintia, 80126 Napoli
ITALY

Joint ITER-IAEA-ICTP
Advanced Workshop on "Fusion and Plasma Physics"
Trieste, October 3 - 14, 2011

Dust in tokamaks

U. de Angelis

University of Naples and INFN Sezione di Napoli, Napoli, Italy

C. Castaldo

Euratom ENEA Association, Frascati, Italy

M. De Angeli, E. Lazzaro

Istituto di Fisica del Plasma, CNR, Milan, Italy

D. Jovanovic

Institute of Physics Belgrade, Belgrade, Serbia

C. Marmolino

Department STAT, University of Molise, Pesche (IS), Italy

S. Ratynskaia

Royal Institute of Technology (KTH), Stockholm, Sweden

Outline

- State of the art: what we do and do not know about dust in tokamaks
- Hyper-velocity particles
- Dust dynamics
- Stochastic heating
- Diffusion of a dust cloud
- Blobs
- Scattering of radiation: new diagnostics?

DIAGNOSTICS OF DUST

- **Postdischarge methods are well established: Analysis of particles collected after experimental campaigns**

- **Analysis of deposits showed large spread in dust size from sub-μm to 100 μm**

- **Currently the main challenge is diagnostics of dust *during the discharge***

- **Dust parameters of interest: (apart from material), size, velocity and number density**

DIAGNOSTICS DURING DISCHARGES

- **Visible imaging**
  - **Few hundreds m/s for a bright dust grain of few μm**
  - **Individual particle observed with velocities up to 500 m/s**

- **Capture by porous aerogel targets**
  - **For both slow and fast dust**

- **Light scattering**
  - **No information on velocity**
  - **JIPPT-IIU after disruption, radius 0.4-1 μm** K. Narihara *et al*. 1997 NF **37** 1177
  - **DIII-D SOL during discharge, 6 10^3 m^{-3}, radius 80-90 nm** W. P. West *et al 2006* PPCF, **48**, 1661
  - **FTU after disruptions, 10^7 m^{-3}, radius 50 nm** E. Giovannozzi *et al.* 2007 AIP Conf. Proc. Vol. 988, pg. 148
  - **densities of nano-particles of order 3x10^7 cm^(-3) are consistent with observations** S.I.Khrasheninnikov, T.K.Soboleva and D.H.Mendis in Proc. 19th PSI Conf., San Diego, 2009

AEROGEL IN

SPACE

(mm scale on figures below)

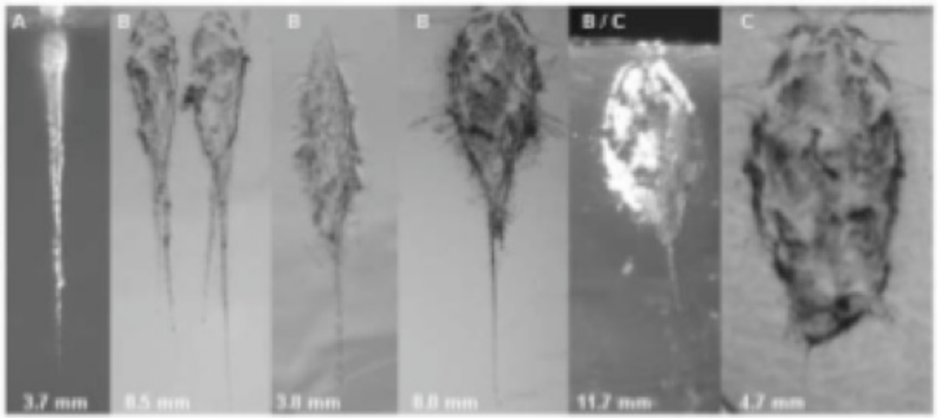

Stardust, 1999-2004

AFTER: F. Hortz *et al.* 2006 Science 314

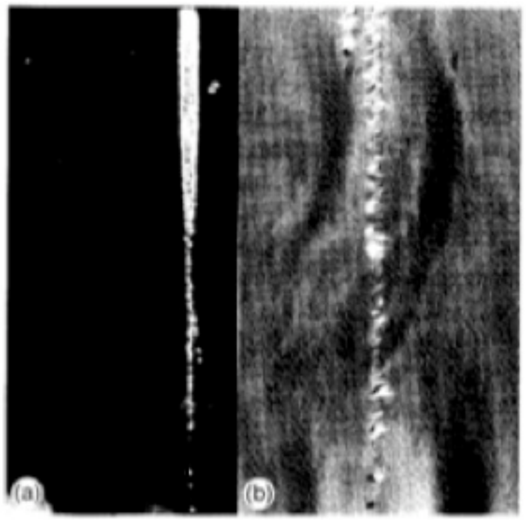

Shuttle, 1992

AFTER: P. Tsou 1995
Journ. Non.Cryst. Solids
186 415

TOKAMAKS

Aerogel compatibility with tokamak operation

Ratynskaia S. *et al* 2008
PPCF **50** 124046

FIRST EXPOSURES

- **HT-7 tokamak**

  Morfill G. E. *et al*. 2009
  New J. Phys. **11** 113041

- **TEXTOR tokamak**

  Ratynskaia S. *et al*. 2009
  Nuclear Fusion **48** 122001

- **EXTRAP reversed-field pinch**

  Bergsåker H. *et al*. 2010
  J. Nuclear Materials

RESULTS OF DUST CAPTURE BY AEROGEL IN TEXTOR

S. Ratynskaia, H. Bergsåker, B. Emmoth, A. Litnovskiy *et al* 2009 NF **49** 122001

- **First time-resolved measurements**
- **Most of the dust of ohmic discharges was collected during the flat-top phase**
- **Particle flux density of 20-50 particles cm^{-2} s^{-1}, for particles that were sufficiently big to be visible optically (> 6 μm) and sufficiently fast (~ 100 m/s) to stick to the surface.**
- **Fast dust is more rare**

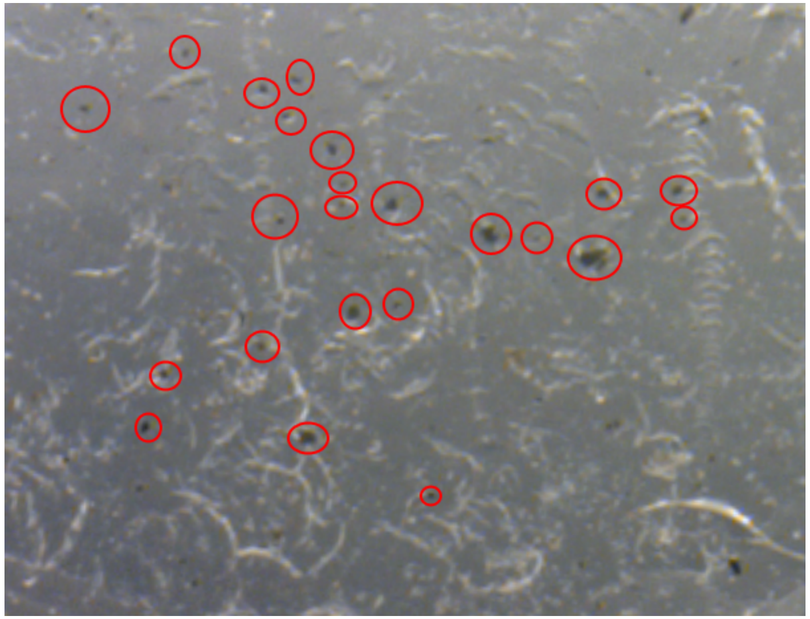

DUST IMPACT IONIZATION IN FTU TOKAMAK

C Castaldo *et al* 2007 Nuclear Fusion **47** L5
S. Ratynskaia *et al* 2008 Nuclear Fusion **48** 015006

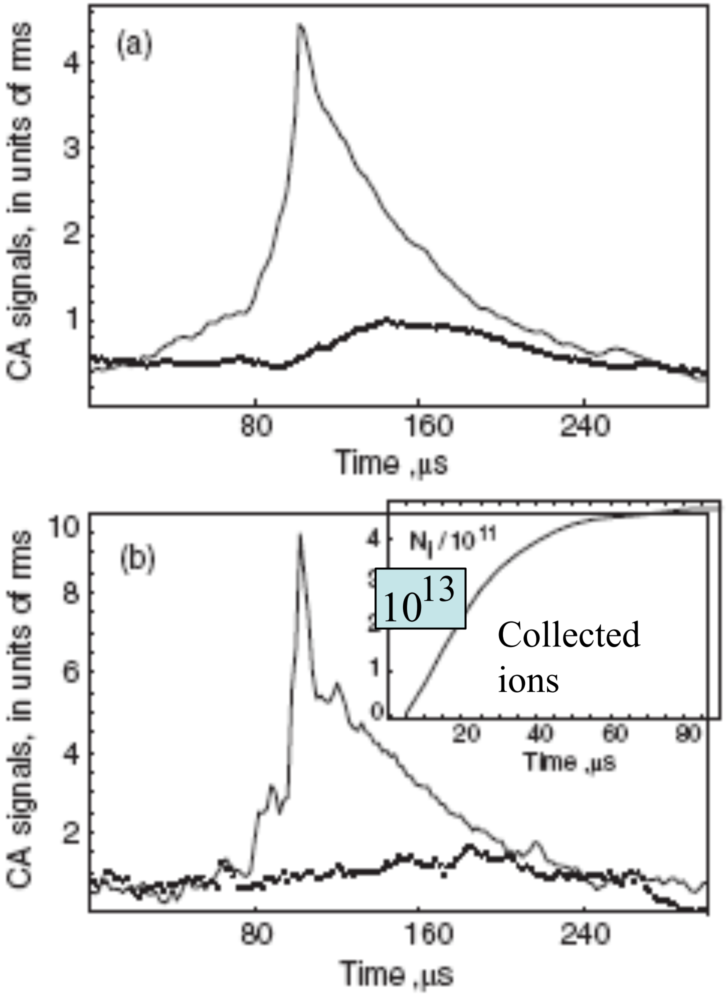

charge 10^{11}-10^{13} e upon impact of ~1 μm Fe particle on Mo surface with velocity of few km/s

Burchell M. *et al* 1999 Meas. Sci. Technol. 10 41

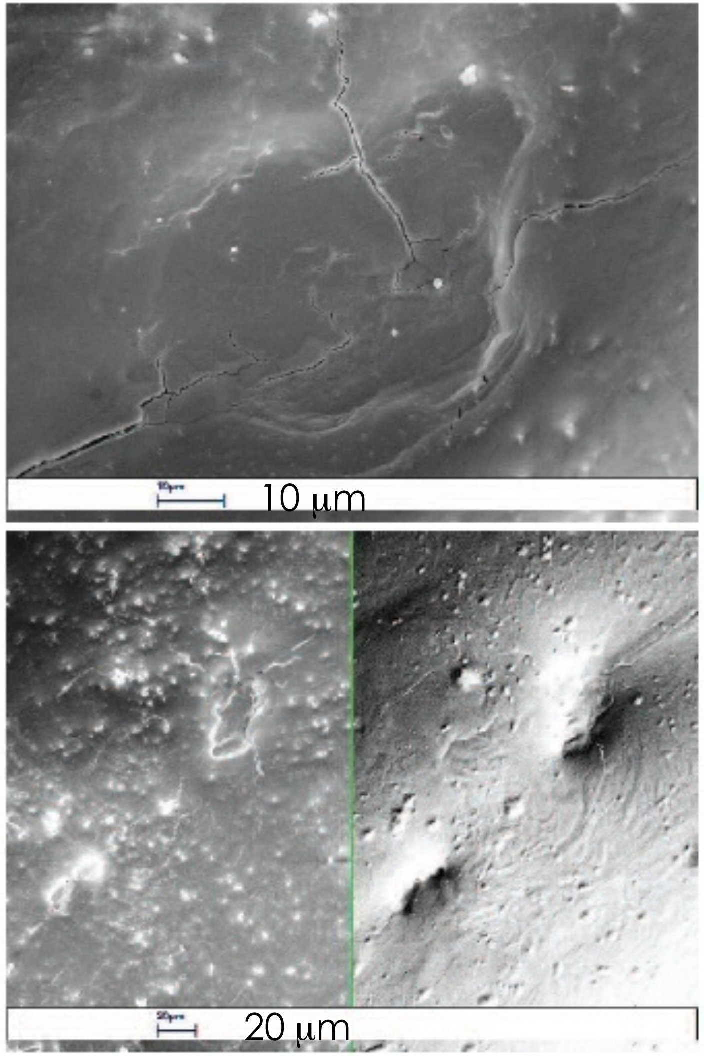

Impact craters

DUST IMPACT IONIZATION-FOR RARE FAST DUST

- For most materials the hypervelocity regime (when the impact speed > the speed of the compression waves both in the target and projectile) has been reached when the impact speed exceeds 2-3 km/s
- The resulting pressure can reach 1 TPa and the temperature can be sufficient to cause vaporization and ionization of the materials.
- Diagnostics based on the phenomenon:
  – (i) charge released (ii) craters on the target surface
- Laboratory studies of impacts [M. J. Burchell et al, Meas. Sci. Technol. 10, 41 (1999).]
  – charge 10^{11}-10^{13} e upon impact of ~1 μm Fe particle on Mo surface with velocity of few km/s
  – (with t = 10-100 ms) ~10 mA current – feasible to measure in SOL
- Probe measurements in FTU near the wall, equatorial plane

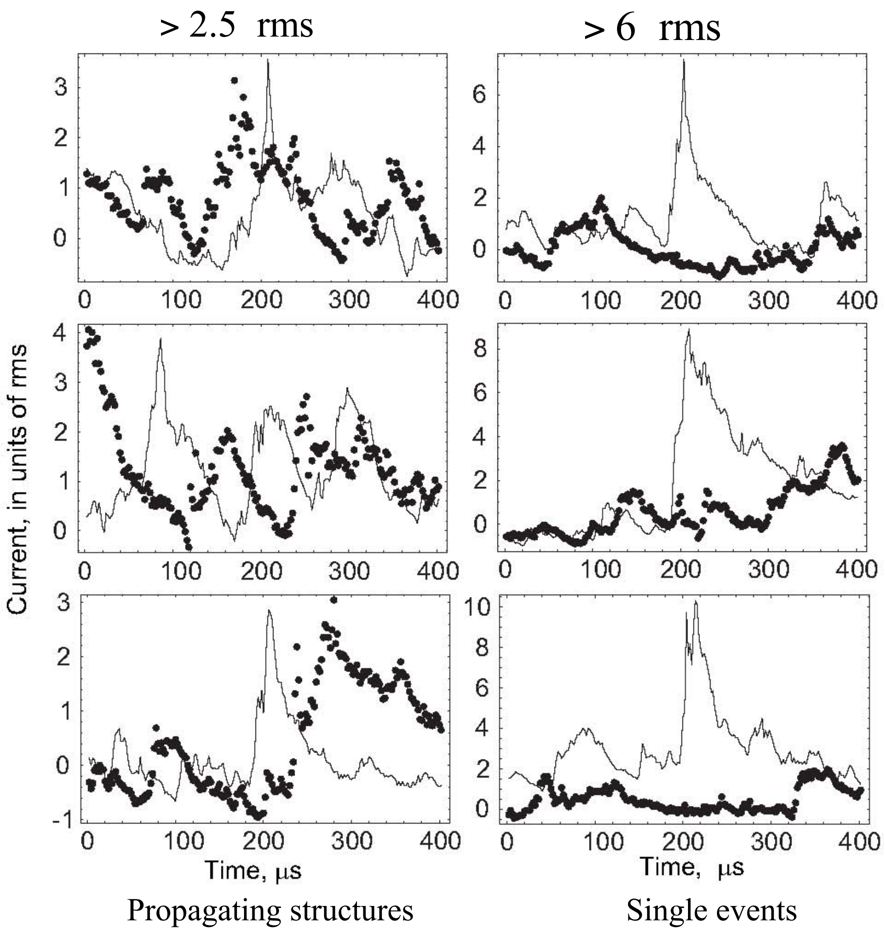

- Two equatorial probes (separation 0.6 cm)
- Lack of correlation, expecially for largest fluctuations
- Very rare extreme events
- Rate increases towards walls

DUST IMPACTS - CRATERS ON THE TARGET SURFACE

- Dimensions of the craters are function of the projectile parameters – empirical results available

- Craters smooth, no rough rims from ejected molten metal typical for the unipolar arcs

- Cracks observed - not typical for the arcs where surface damage is due to heating by the arc current

- Arc hops and leaves scratches on mm scale- none were found

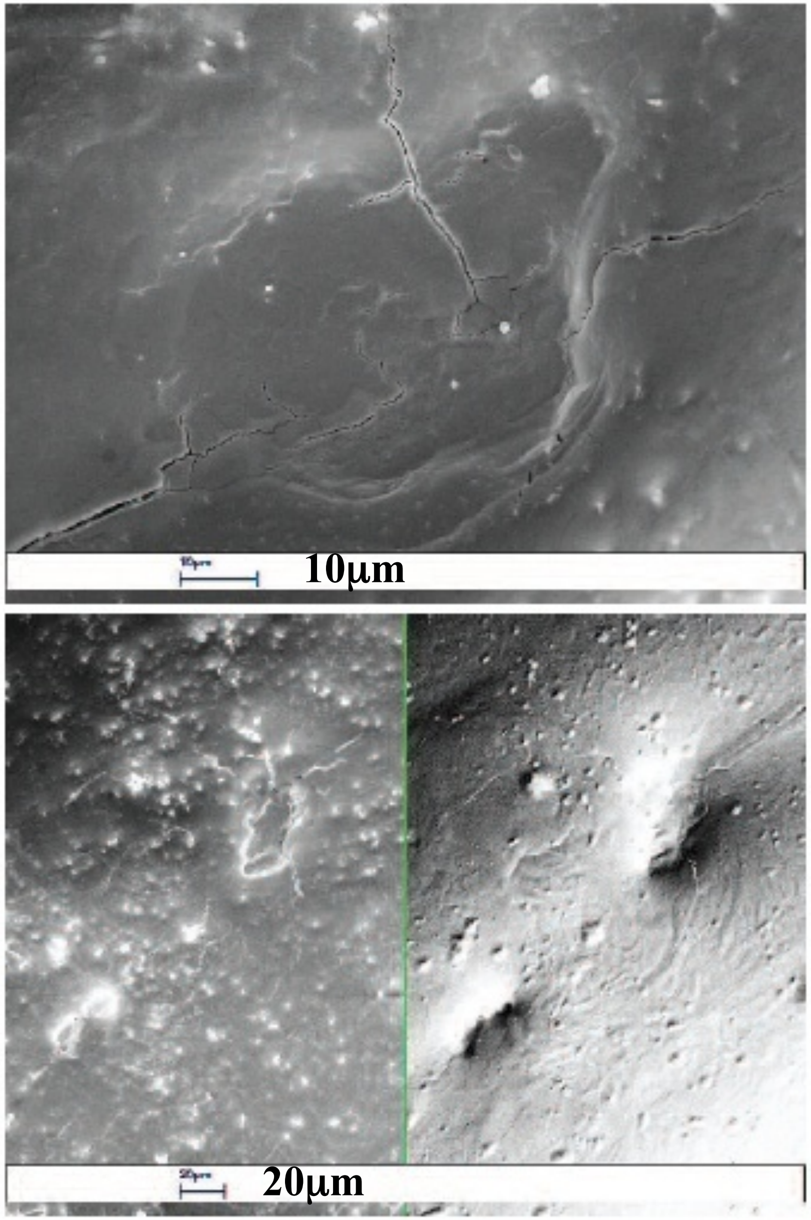

DUST IMPACT PHENOMENA VS ARCS

- Probe current spikes are < 50 mA

The unipolar arcs are characterized by a threshold current ~1 A, necessary to sustain the arcs

B. Juttner 2001 J. Phys. D 34 R103

Crater morphology;

- Characteristic scale – 10-100 microns
- The rough rims from ejected molten metal (typical for unipolar spots) are missing
- The arc hops from one spot to another causing several mm scratches - not observed

COMBINATION OF ELECTRIC MEASUREMENTS WITH OPTICAL

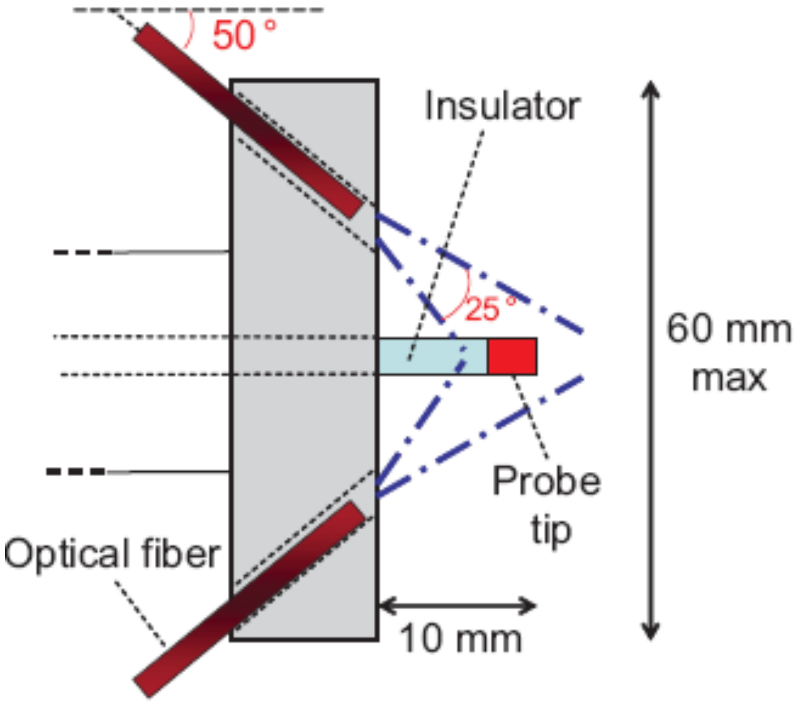

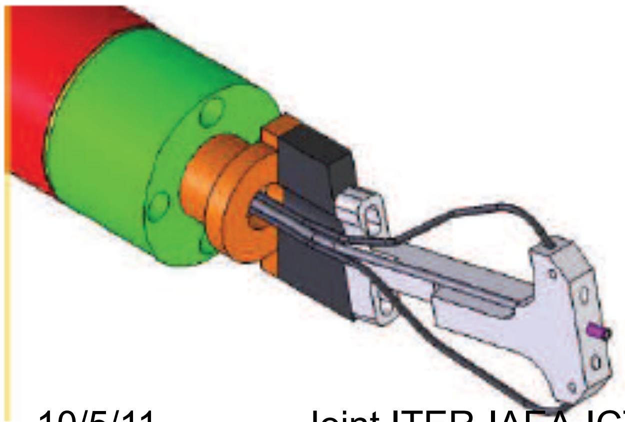

To discriminate dust impact ionization events from features due to collective plasma structures (blobs)

simultaneous detection of

- Charge released

and

- Line emission at a target material wavelength

Castaldo C. *et al* 2010 PPCF **52** 105003

Hypervelocity Particles in Fusion Devices

- Numerical codes for micron-size particles: Visible imaging

$$v \le 200 \;\; m/s$$

- Rudakov D. 2007 *1st Workshop on Dust in Fusion Plasmas* (http://cpunfi.fusion.ru/eps-dust-media2007/Rudakov.....S1-3)

$$\text{DIII-D size} \;\; \ge 10\mu m, \;\; v \ge 0.5 km/s$$

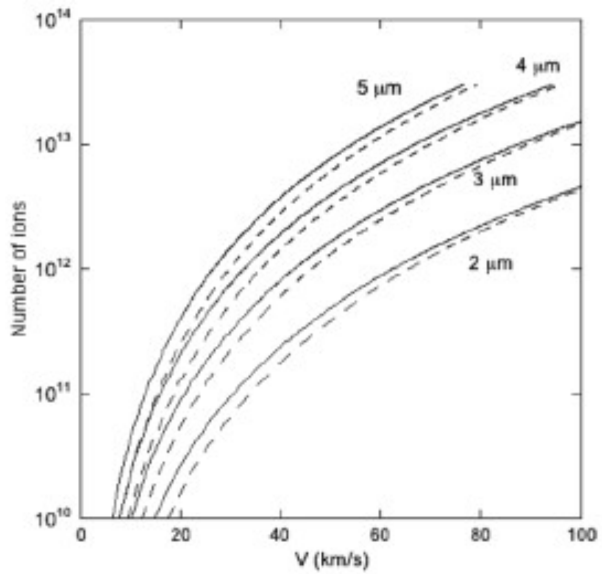

Figure 1. Results of the empirical expressions of [2]: number of ions produced upon impact of an iron projectile on a molybdenum surface target as a function of the projectile velocity and radius. The dashed line corresponds to the fast and the full line to the total ionization. See text for definitions.

FTU: few km/s, micron-size particles

$\rightarrow$

IMPACT IONIZATION

Dynamics of dust in gap edge plasma-first wall

Typical profiles in plasma-wall gap and main forces on dust

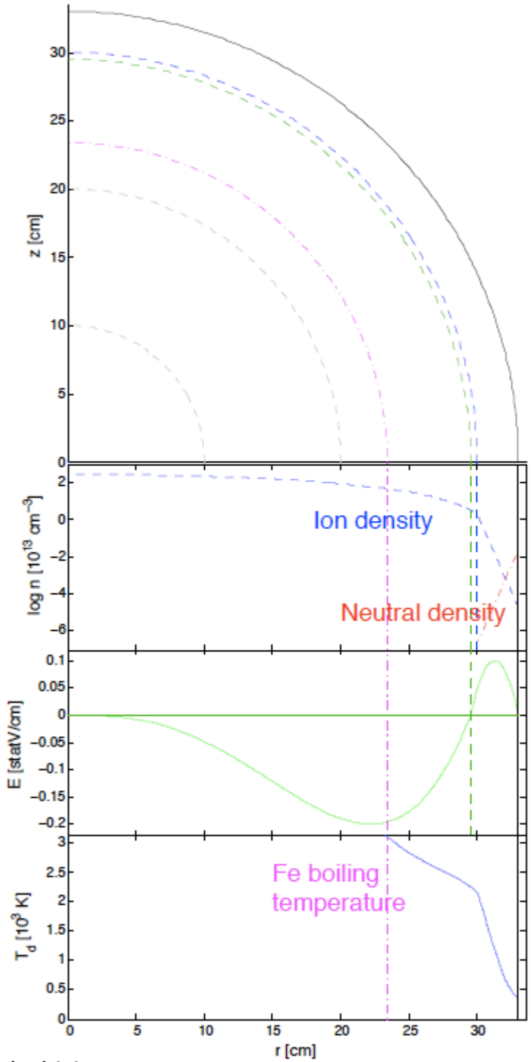

Isolated Fe Dust particles' motion

$$\begin{cases} \frac{d\mathbf{r}}{dt} = \mathbf{v} \\ \frac{dM_d\mathbf{v}}{dt} = \mathbf{F}_{fric,i} + \mathbf{F}_{fric,n} + \mathbf{F}_E + \mathbf{F}_{v\times B} + \mathbf{F}_{\nabla B} + M_d\mathbf{g} + \Theta_{d,w} \end{cases}$$

Ion-drag force:sling shot effect

$$\mathbf{F}_{fric,\alpha} = \xi_\alpha \xi_{fric,\alpha} m_\alpha n_\alpha v_{th,\alpha} \left(\mathbf{V}_\alpha - \mathbf{v}\right) \sigma_d$$

Quasiselastic reflections from the wall up to

$$V_d \leq 1km/s$$

Periodic reinjection in acceleration layer

Example of acceleration of a 4μm(diameter) Fe dust particle in FTU with a single wall collision

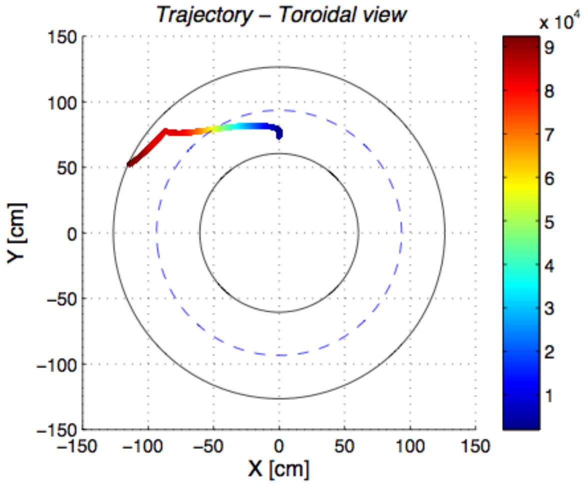

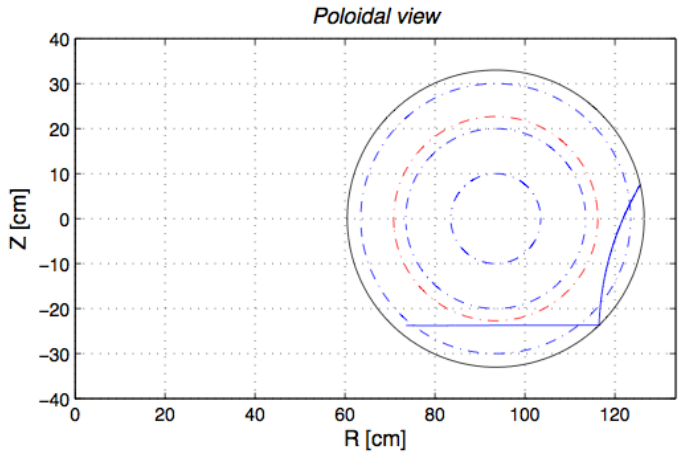

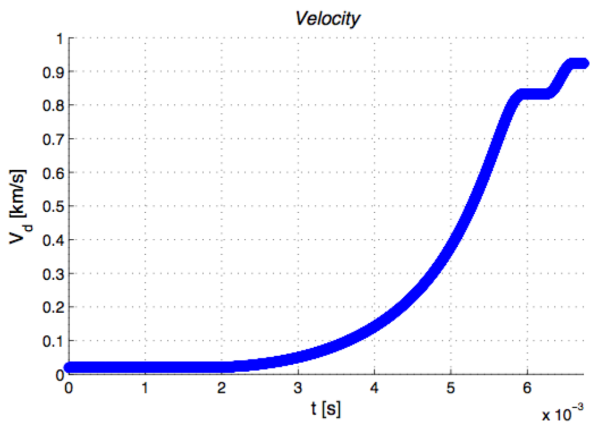

Example of acceleration of a 4μm Fe dust particle in FTU with few wall collision

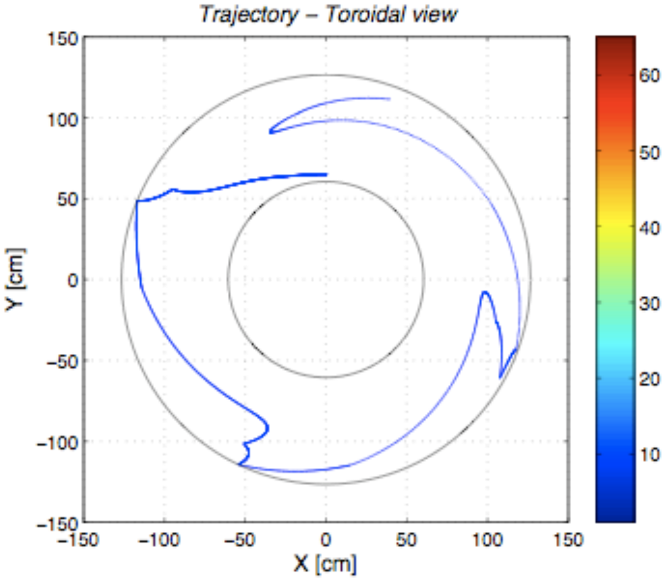

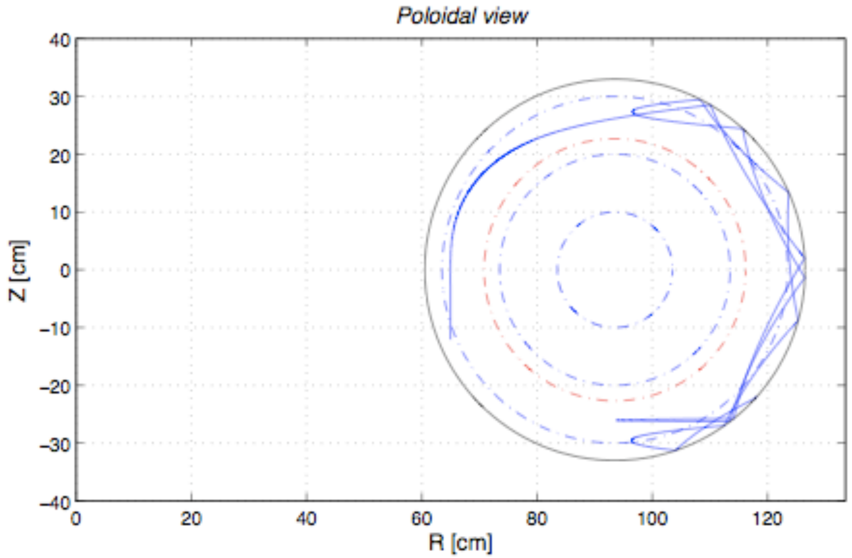

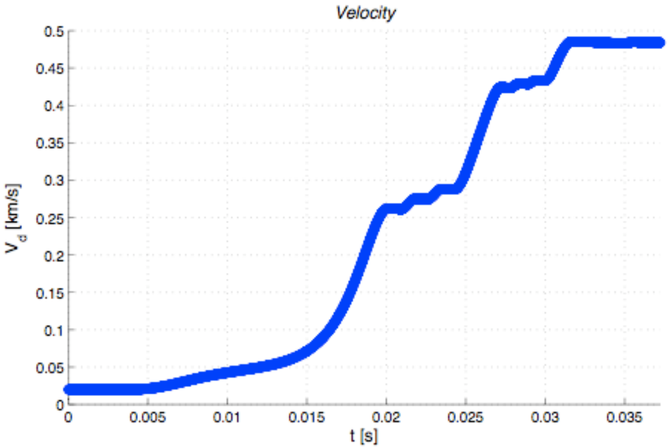

- Last velocity = 0.50 km/s

Example of acceleration of a 4μm Fe dust particle in FTU with 10^2 wall collision

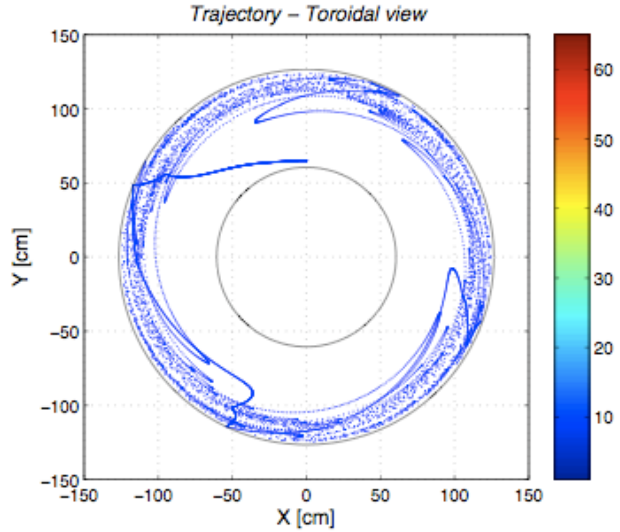

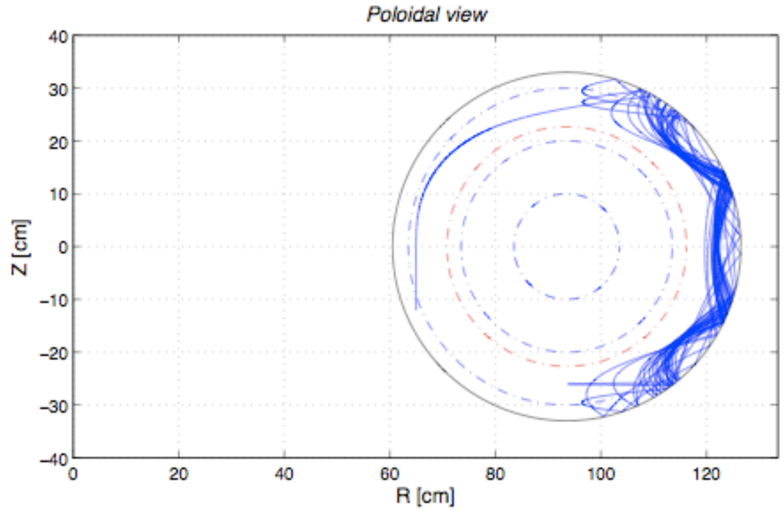

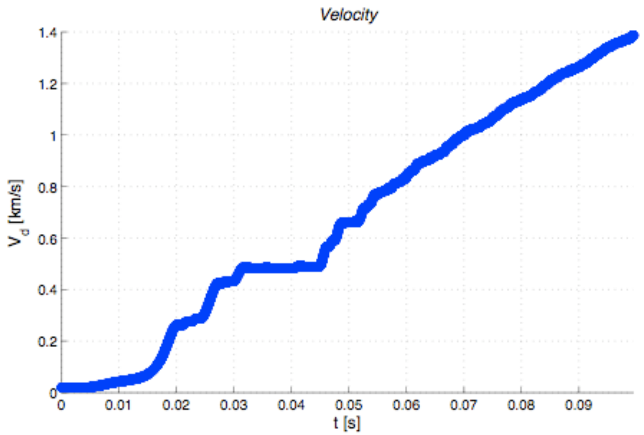

Exit parameters:

- Exit time = 0.10 s
- Diameter = 3.62 um
- Reflections = 101
- Last velocity = 1.39 km/s
- Last Larmor radius = 24282.04 cm
- Max inward pos = 24.61 cm
- Max dust temp = 2731.86 K

Example of “racetrack Billiard” acceleration of 2μm Fe dust particle in FTU by ion drag and N wall collisions*

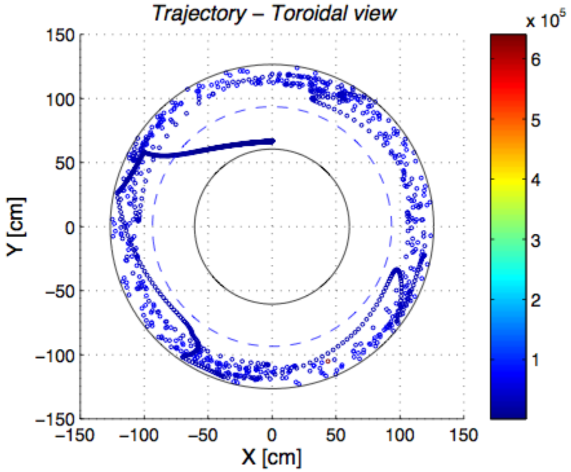

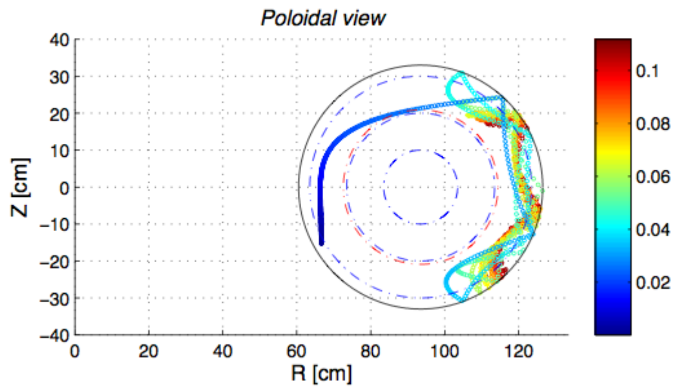

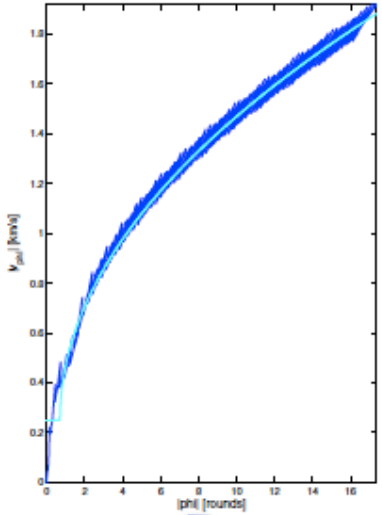

Final fragmentation upon collisionleads to fragment speed ~7 km/s

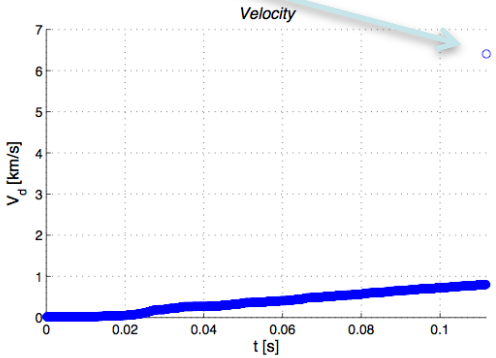

In *FTU geometry* V_{max}~$(LN)^{0.5}$;
- L is the ion drag interaction length

[*] I. Proverbio, E.Lazzaro et al, in print PPCF 2011

Stochastic Heating

Dust charge fluctuations $\longrightarrow$ non conservation of energy in dust-dust interaction

$$\varepsilon = \frac{1}{2} m_d \int v^2 \Phi^d(v) d^3 v \qquad \frac{d\varepsilon}{dt} = \nu\varepsilon \qquad \nu \cong \frac{\omega_{pd}^2}{\nu_{ch}} \frac{1}{Z_d}$$

1) From the self-consistent kinetic description of dusty plasmas

de Angelis U *et al* *Physics of Plasmas* **12**(5) 052301 2005

$$\frac{d\Phi^d}{dt} = I_C + I_{NC}$$

2) From a Fokker-Planck approach to systems with variable charge

Ivlev A V *et al* *Physics of Plasmas* **12**(9) 092104 2005

$$\frac{d\Phi^d}{dt} = St_{dd} F^M + St_{dn} F^M$$

3) As an energetic instability of a harmonic oscillator with random frequency

Marmolino C *Physics of Plasmas* **in print** 2011

$$\frac{d^2 x(t)}{dt^2} = -\frac{4\pi n_d q^2(t)}{m_d} x(t) \; ; \qquad \frac{d\langle \varepsilon(t) \rangle}{dt} = \nu \langle \varepsilon(t) \rangle$$

Two Step Model

Nanoparticles are stochastically heated and transfer energy to microparticles via collisions:
For the case of dissipation on ions with energy Ti.

$$\frac{d\varepsilon}{dt} = \nu\varepsilon - 2\gamma_n\left(\varepsilon - \frac{3}{2}T_i\right) \qquad \text{nanoparticles}$$

$$\frac{dE}{dt} = \Gamma\varepsilon^{1/2}\left(\varepsilon - E\right) - 2\gamma_\mu\left(E - \frac{3}{2}T_i\right) \qquad \text{microparticles}$$

Geometrical cross-section

$$\Gamma = n_d \frac{\sqrt{m}}{M}\pi A^2$$

Condition for growth

$$\nu_{eff} = \nu - 2\gamma_n > 0$$

Marmolino C, de Angelis U, Ivlev A & Morfill G E, AIP Conf. Proc. **1061**, 105 (2008)
Marmolino C, de Angelis U, Ivlev A & Morfill G E, Phys. Plasmas **16**(3), 033701 (2009)

Energy growth (FTU-SOL conditions)

a) $\nu_{eff} > 0$

$$\frac{\varepsilon(t)}{\varepsilon_o} = e^{\nu_{eff}t} + \frac{3\gamma_n T_i}{\nu_{eff}\varepsilon_o}\left(e^{\nu_{eff}t} - 1\right)$$

b) $\nu_{eff} < 0$

$$\frac{\varepsilon(t \to \infty)}{\varepsilon_o} = \frac{3\gamma_n T_i}{|\nu_{eff}|\varepsilon_o}$$

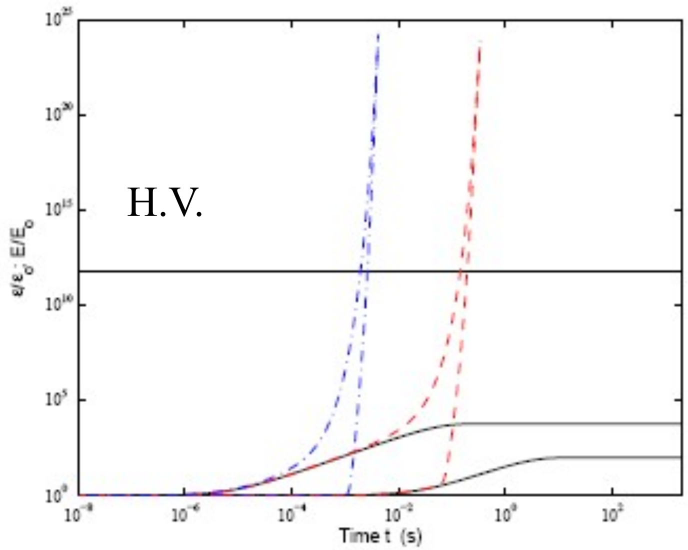

FIGURE 2. The normalized energy of the nano (ε) and micronsize (E) particles versus time in seconds, for different values of the density of the nanoparticles. For each pair, the curve for ε is the one with earlier growth. Full line $n_d = 5.3 * 10^4$ cm^{-3} (below the instability threshold, corresponding to $n_d = 5.3905 * 10^4$ cm^{-3}); dashed line $n_d = 6. * 10^4$ cm^{-3}; dot-dashed $n_d = 6. * 10^5$ cm^{-3}.

Diffusion and S.H. of a dust cloud

Marmolino C, Bacharis M, Allen J E, de Angelis U, Willis C, Phys. Plasmas **in print** (2011)

- a cloud of nm dust particles forms near the wall;
- spherical clouds are used here for analytical estimates: "small" (r < 3 cm = FTU SOL linear dimension) and “large” spherical clouds.
- the Orbit Limited Motion (OML) approximation is used to calculate Q_d and the diffusion approximation is valid
- $n_d < 10^9$ p/cm^3 and neutrality.

Cloud diffusion

$$\frac{\partial n_d(r,t)}{\partial t} = \frac{D}{r^2}\frac{\partial}{\partial r}\left[r^2\,\frac{\partial n_d(r,t)}{\partial r}\right]$$

$$D = \frac{k_B T_i}{m_d \gamma_i} \cong 2\times 10^5\ \frac{\mathrm{cm}^2}{\mathrm{sec}} \qquad \text{FTU SOL plasma and } a_g = 5\ \mathrm{nm}$$

Initial condition, a spherical cloud with a gaussian dust distribution

$$n_d(r,t=0) = \frac{N_d}{\left(2\pi r_o^2\right)^{3/2}}\,Exp\left(-\frac{r^2}{2r_o^2}\right)$$

The radius evolution

$$\bar{\mathrm{r}}(t) = \frac{\int r n_d(r,t)\,dV}{N_d} = r_o\sqrt{\frac{8}{\pi}\left(1+\frac{2D}{r_o^2}t\right)}$$

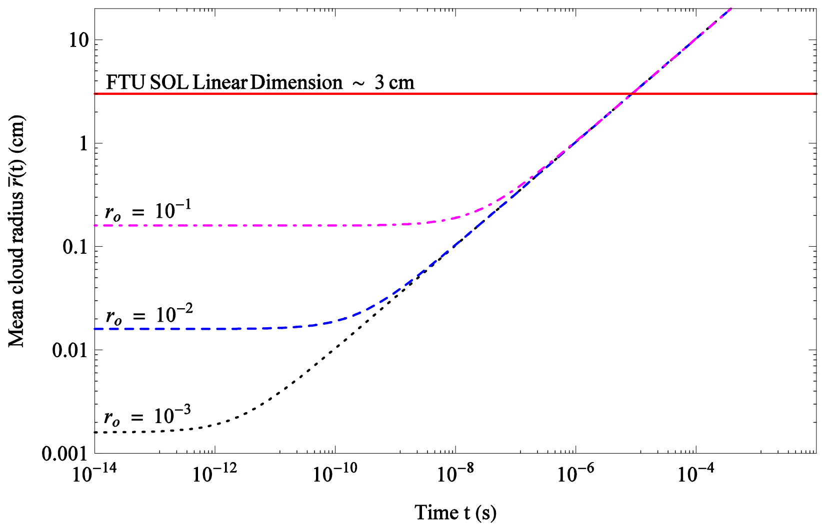

The S.H. of a diffusing cloud

$$\frac{d\varepsilon(t)}{dt} = \left[\nu - 2\gamma_i\right]\varepsilon(t) + 2\gamma_i \varepsilon_i$$

$$\nu(r,t) = \frac{1}{Z_d}\frac{\omega_{pd}^2}{\nu_{ch}} = \frac{1}{Z_d}\frac{4\pi q_d^2}{m_d \nu_{ch}} n_d(r,t)$$

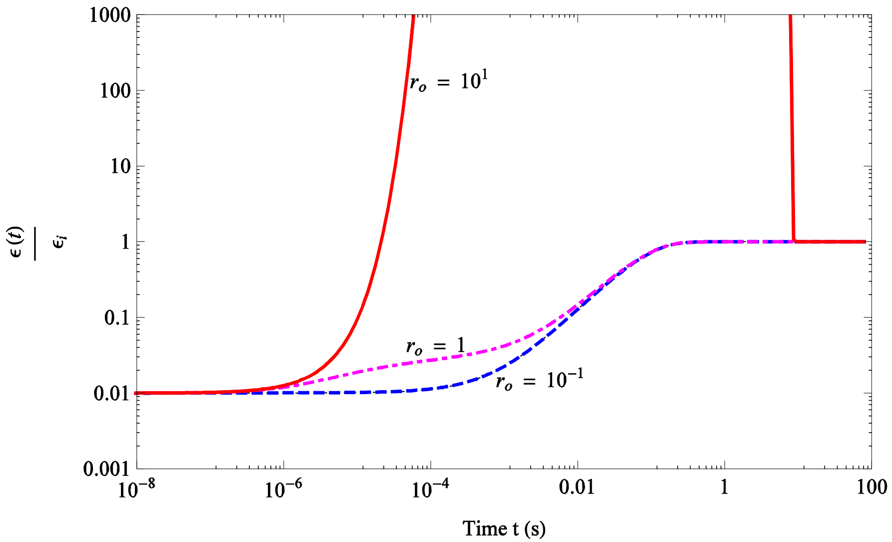

Plasma blobs

- Blobs are long-lived quasi-coherent structures, created at the edge of the tokamak core by the turbulence in the unfavorable curvature region, driven by the unstable interchange and ballooning modes.
- Plasma blobs are strongly elongated along the magnetic field, in the form of filaments. They start as the avalanches of the hot and dense core plasma across the last closed magnetic surface into the cold and tenuous SOL region.
- Their dynamical properties are governed by the dissipations, including processes at the contact with the conductive wall.
- Experimentally, blobs are easily detected by Langmuir probes at the tokamak wall. They produce spiky electrostatic signals.
- Effects of dust on Blob dynamics

D. Jovanović, U. de Angelis, *et al* Phys. Plasmas **14**, 083704 (2007)

Dimensionless equations

Electron continuity:

$$\left[\frac{\partial}{\partial t} + (\vec{e}_z \times \nabla\phi)\cdot\nabla\right] n_e = \nabla_\perp\left(D\nabla_\perp n_e\right) - \sigma n_e,$$

Charge continuity:

$$\nabla_\perp \cdot \left\{ n_i \left[\frac{\partial}{\partial t} + (\vec{e}_z \times \nabla\phi)\cdot\nabla\right] \nabla_\perp\phi \right\} - \frac{\partial n_e}{\partial y} =$$

$$n_i\,\chi_0\,\phi - \nabla_\perp\cdot\left[n_i\left(\chi_2 - \chi_4\,\nabla_\perp^2\right)\nabla_\perp\phi\right].$$

χ_0 - *losses to the tokamak wall*

χ_2 - losses due to *ion-dust collisional*,

χ_4 - *viscous* losses

Radial propagation of blobs

Collapse into a thin shell (all sizes of blobs) in the absence of dissipations

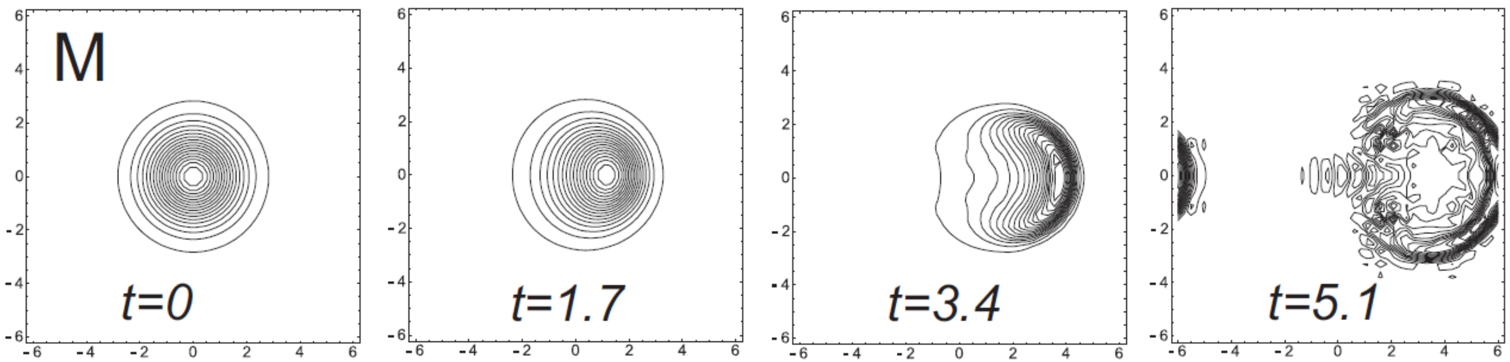

Collapse into a shell and spatial shrinking of small blobs due to viscosity:

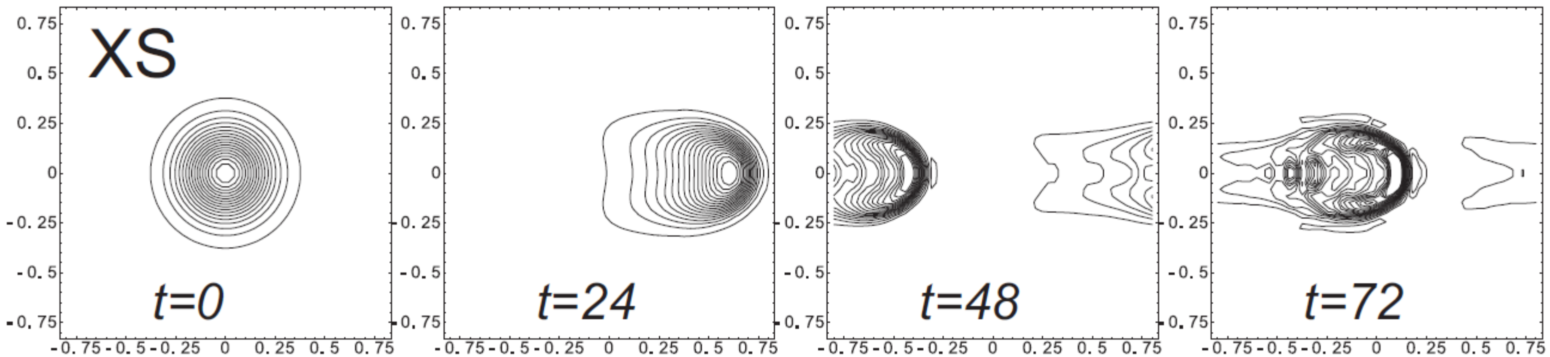

Radial propagation of blobs

Raleigh-Taylor instability (fingering) of large blobs by losses to the wall

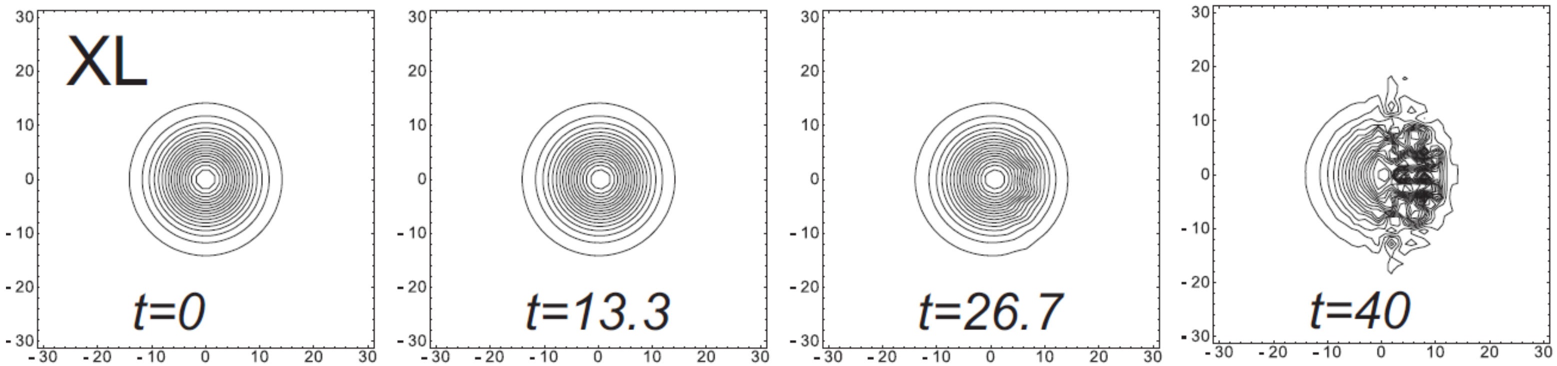

Dissipation of blobs due to ion-dust collisions

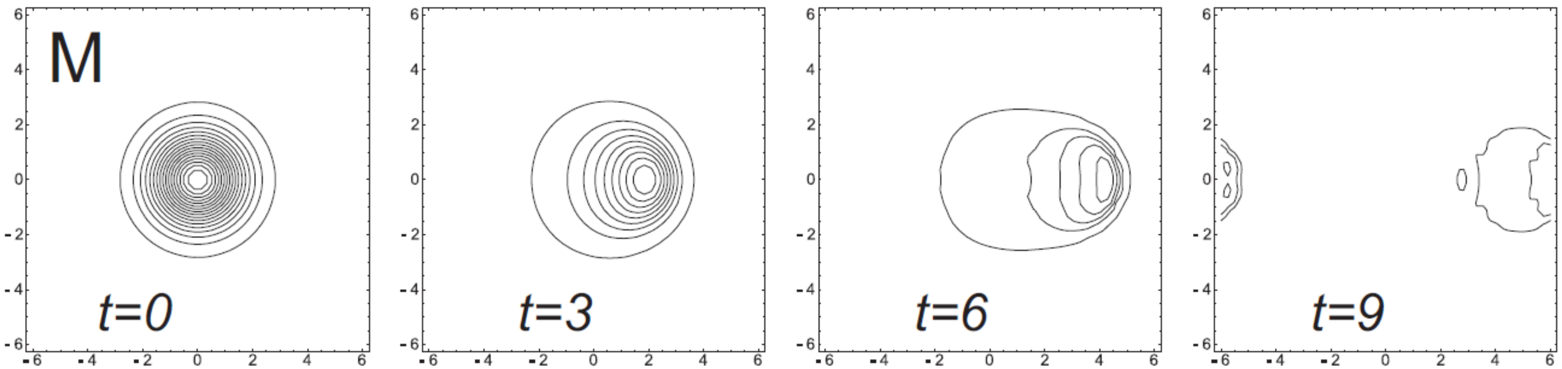

Maximum radial distance travelled by a blob

Typical solution (in DIII-D tokamak) for the maximum excursion, as a function of the blob size L and the ratio P of the total dust and electron charge densities.
Losses to the dust (green),
Losses to the wall (red),
No losses (blue)

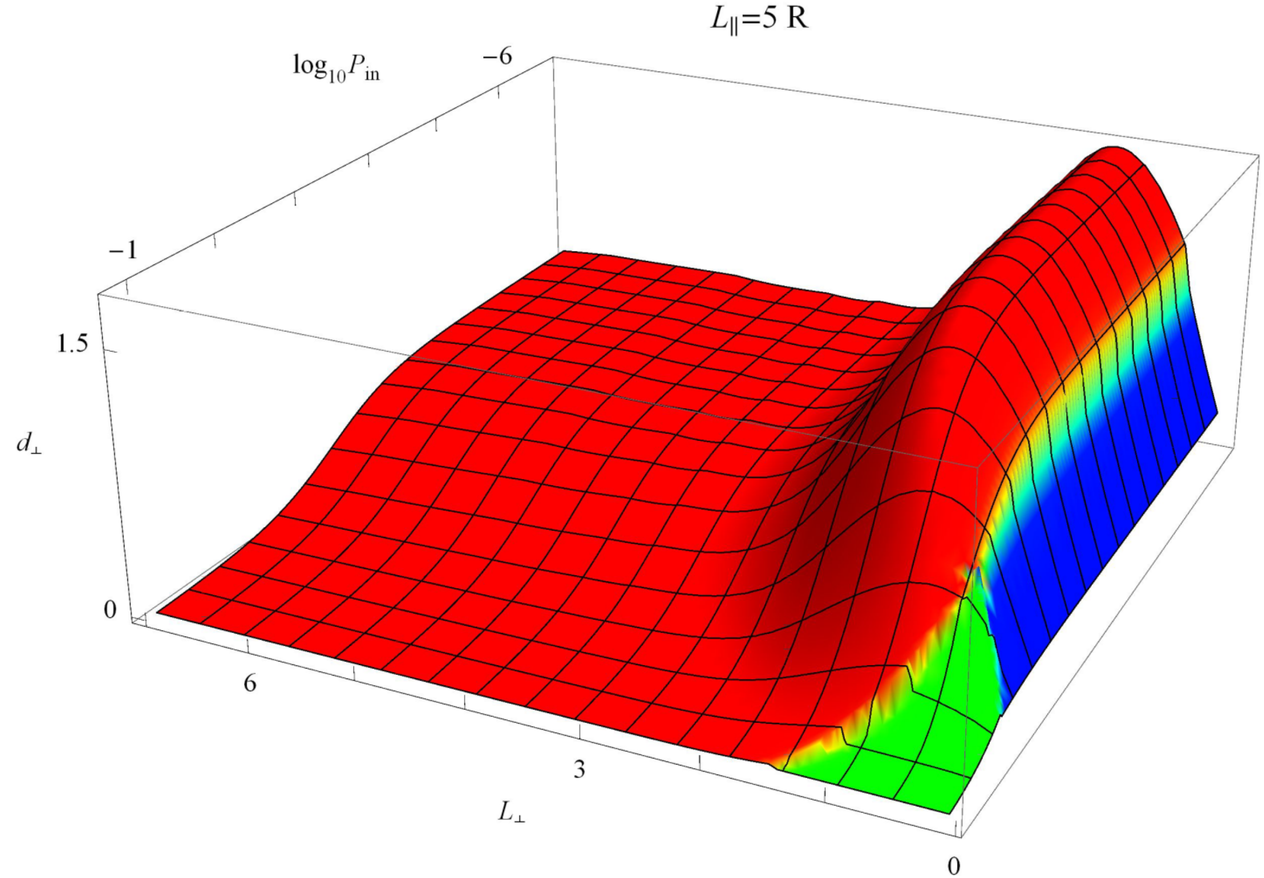

Amount of 30 nm dust that dissipates the blob before reaching the wall

The minimum dust number density, and the minimum amount of dust in the entire scrape-off layer that dissipate the blobs before they reach the wall.

Machine	z_d	ζ	ν_{ch}	$P_M^{(in)}$	$P_T^{(in)}$ $(L_\parallel = 5R)$	Threshold dust number density $n_{d,T}$	Threshold dust specific gravity $\rho_{d,T}$	Total dust mass at threshold $M_{d,T}$
C-Mod H	1317	2.75	20.8 MHz	0.63	0.016	1.68×10^{14} m^{-3}	35.8 g/m^3	3.26 g
C-Mod L	1269	2.77	33.5 MHz	0.13	0.010	1.73×10^{14} m^{-3}	36.8 g/m^3	3.36 g
DIII-D	577	2.77	22.6 MHz	0.15	0.0063	1.09×10^{14} m^{-3}	23.2 g/m^3	14.27 g
JET	2556	2.73	10.6 MHz	1.22	0.016	0.62×10^{14} m^{-3}	13.2 g/m^3	38.13 g
NSTX	751	2.77	11.9 MHz	0.04	0.010	0.80×10^{14} m^{-3}	16.9 g/m^3	5.81 g
T-10	866	2.77	55.4 MHz	0.09	0.003	1.10×10^{14} m^{-3}	23.3 g/m^3	8.06 g
TCV	1155	2.77	32.0 MHz	0.08	0.005	0.87×10^{14} m^{-3}	18.5 g/m^3	2.43 g

TABLE II: The parameters of the dust fluid, in the case of dust grains with the radius $a = 30\,\mathrm{nm}$.

Just 3 – 30 g of nanometer-sized dust in the entire SOL is sufficient to prevent the blobs from reaching the wall. This may provide a new method for the detection of nanometer dust.

Main effects of dust particles in plasmas

*V. N. Tsytovich, U. de Angelis, Phys Plasma **6**, 1093 (1999).*
*V. Tsytovich, G. Morfill, and H. Thomas, Plasma Phys. Rep. **30**, 816 (2004).*

- dust represents new dissipation by continuously collecting plasma (electron and ion) fluxes

- thus an inclusion of a source is necessary to define a steady-state in such systems

- fluctuations in the collected fluxes lead to fluctuations of the dust charge

- dust discreteness plays an important role even in cases where continuous (Vlasov) description for electrons and ions is sufficient

Modifications of plasma responses as potential dust diagnostic

- Modification of the plasma density fluctuations implies

- changes in the amplitude and spectrum of their respective (α = {i, e}) correlators

$$S^{\alpha}_{\mathbf{k},\omega} = \left\langle \delta n^{\alpha}_{\mathbf{k},\omega} \delta n^{\alpha *}_{\mathbf{k},\omega} \right\rangle$$

- modified radiation scattering

  V. N. Tsytovich, U. de Angelis, R. Bingham, J. Plasma Phys. ***42****, 429 (1989).*
  U. de Angelis, R. Bingham, A. Forlani. V. Tsytovich, Phys. Scr. ***T98****, (2002).*

- changes of the plasma permittivity $\varepsilon_{\mathbf{k},\omega}$ and hence the plasma modes

- Modification of the Boltzmann equation and the collisional integrals yields modified transport coefficients

  V. N. Tsytovich and U. de Angelis, Phys.Plasmas 11, (2004).

Dust enchances plasma density fluctuations

- ❑ Ion density fluct. spectral density by the multicomponent model

$$S^{i}_{\boldsymbol{k},\omega} = \left\langle \delta n^{i}_{\boldsymbol{k},\omega} \delta n^{i*}_{\boldsymbol{k},\omega} \right\rangle = S^{i(0)}_{\boldsymbol{k},\omega}\left(1 - 2\,\mathrm{Re}\left\{\frac{\chi^{i*}_{\boldsymbol{k},\omega}}{\varepsilon^{*}_{\boldsymbol{k},\omega}}\right\}\right) + \frac{|\chi^{i}_{\boldsymbol{k},\omega}|^{2}}{|\varepsilon_{\boldsymbol{k},\omega}|^{2}}\left(S^{i(0)}_{\boldsymbol{k},\omega} + S^{e(0)}_{\boldsymbol{k},\omega} + Z_d^2 S^{d(0)}_{\boldsymbol{k},\omega}\right)$$

$$\varepsilon_{\boldsymbol{k},\omega} = 1 + \chi^{e}_{\boldsymbol{k},\omega} + \chi^{i}_{\boldsymbol{k},\omega} + \chi^{d}_{\boldsymbol{k},\omega}$$

- ❑ the correlators of the natural density fluctuations of the three species

$$S^{\alpha(0)}_{k,\omega} = \left\langle \delta n^{\alpha(0)}_{k,\omega} \delta n^{\alpha(0)*}_{k,\omega} \right\rangle = 2\pi \int \delta(\omega - \mathbf{k}\cdot\mathbf{v})\,\Phi^{\alpha}(\mathbf{v})\,d\mathbf{v}$$

- ❑ for thermal distributions the correlators take the form $S^{\alpha(0)}_{k,\omega} \propto \dfrac{n_\alpha}{k u_{T\alpha}} e^{-\zeta^2}$

where $\zeta = \dfrac{\omega}{\sqrt{2} k u_{T\alpha}}$

- ❑ for low frequencies $\zeta \approx 1$ we find

$$\frac{Z_d^2 S^{d(0)}_{k,\omega}}{S^{i(0)}_{k,\omega}} \approx P Z_d \left(\frac{m_d}{m_i}\right)^{1/2} \propto a^{7/2}$$

Density correlator (= power spectrum) – measurable plasma observable

- plasma density (α = {i, e}) correlators

  defined as $$S^{\alpha}_{\boldsymbol{k},\omega} = \left\langle \delta n^{\alpha}_{\boldsymbol{k},\omega} \delta n^{\alpha *}_{\boldsymbol{k},\omega} \right\rangle$$

  i.e. the spectral correlation between density fluctuations at point **r** and $\mathbf{r'} = \mathbf{r} + \mathbf{X}$

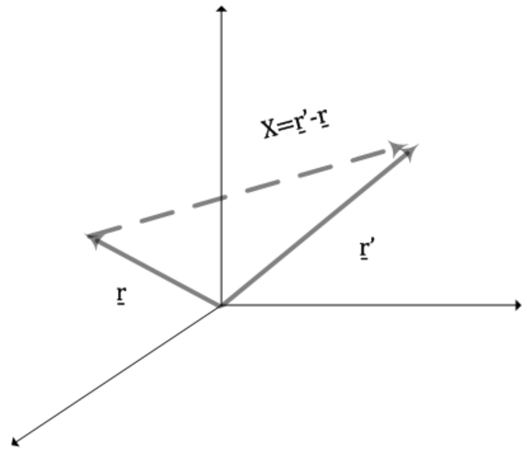

$$S^{\alpha}_{\omega}(\mathbf{X}) = \int S^{\alpha}_{\mathbf{k},\omega} e^{\iota \mathbf{k}\cdot\mathbf{X}} \frac{d\mathbf{k}}{(2\pi)^3}$$

- Typically measured by *single probe* (X=0) as electron/ion saturation currents (under assumption no $T_e,\ T_i$ fluct.), e.g. for ions $\delta N(t) = \frac{I(t) - \bar{I}}{\bar{I}} = \frac{\delta n_i(t)}{n_i}$ so that

$$P_{SD}(f) = \frac{1}{T} \underline{\delta N}(f) \underline{\delta N}^*(f)$$

Power spectra of ion density fluctuations

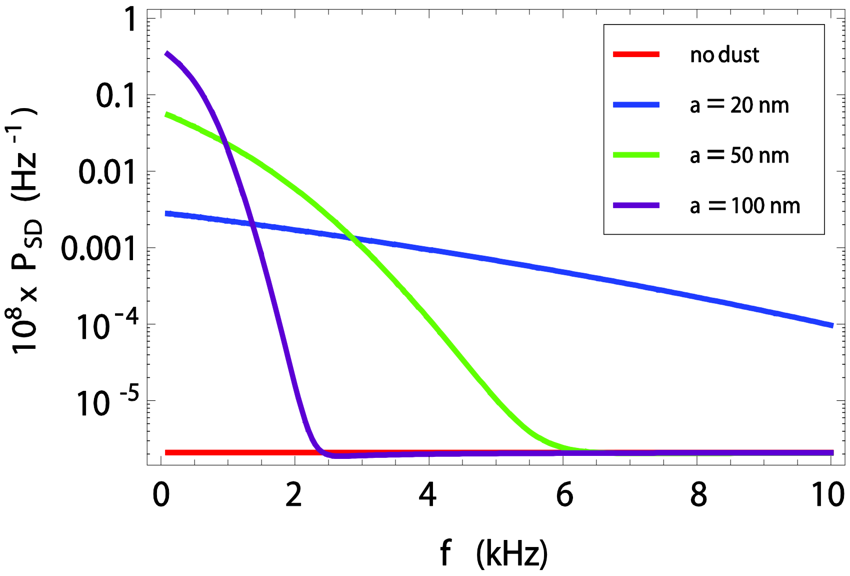

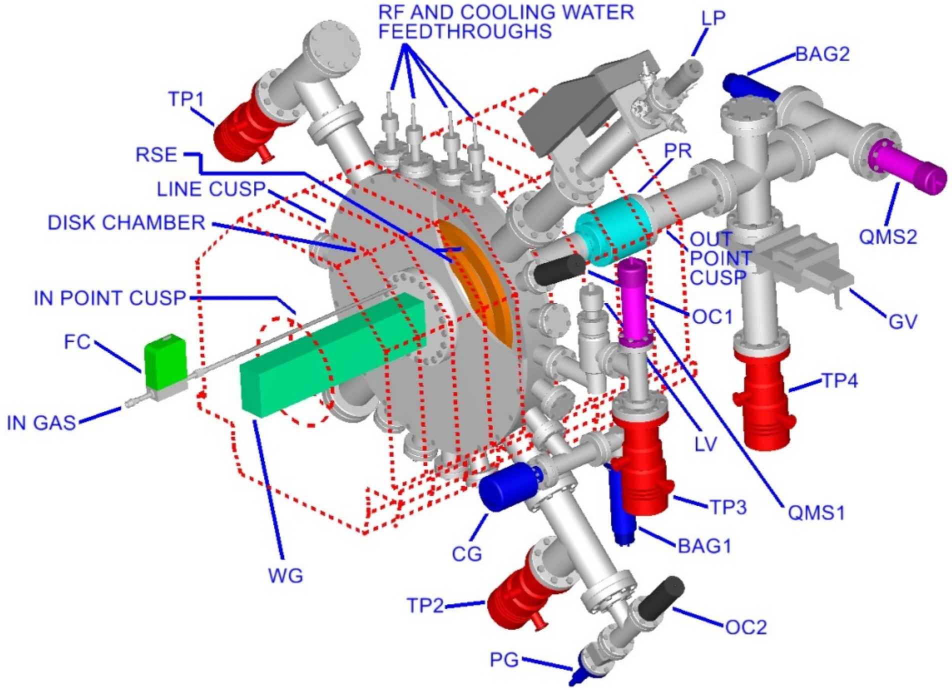

Discharge parameters:

Microwave frequency: f **= 2.45 GHz**
Launcher: Truncated waveguide $TE_{1,0}$
Microwave power: P_{sour} **= 350 W**
Neutral pressure: $P_n = 2\times10^{-3}$ **mbar**
Gas flux: F_g **= 0.45 sccm**

Cusp ratio B_{point}/B_{line} **: 0.3T / 0.19T**
Point to point distance: 78 cm
Line cusp radius: 19 cm

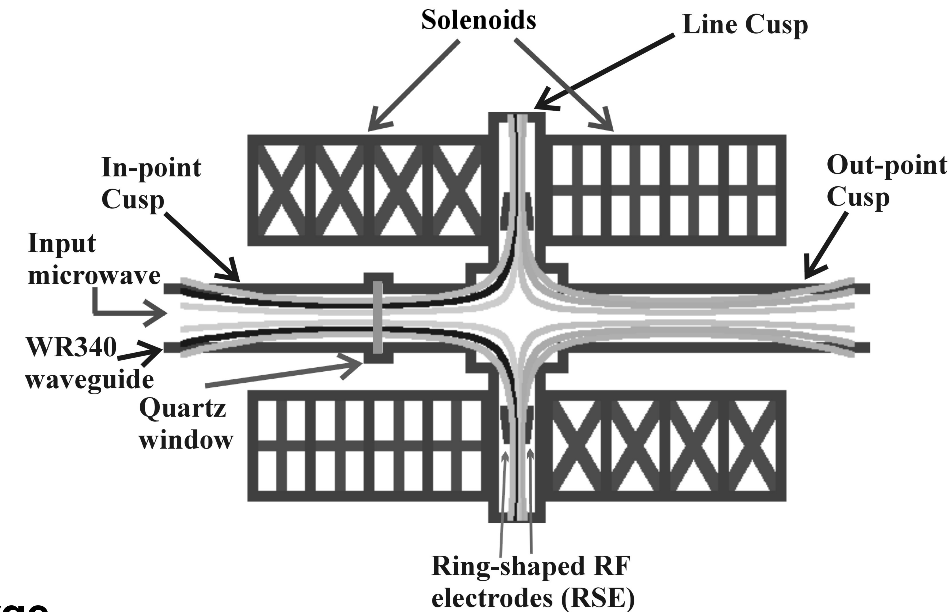

Typical plasma parameters

Plasma density: $n_e \sim 10^{11}$ cm^{-3}
Electron temperature: $T_e \sim 3$ **eV**
Ion temperature: Ti ~ 0.03 eV

Gas mixtures

Ar (dust free)
Ar-NH_3 **(dust free but similar ions with** CH_4**)**
Ar-CH_4 **(carbon dust particles formed)**

For meaningful comparison:

Discharges are similar macroscopically with lowest fluctuation levels achieved in discharge

Results of spectral measurements

"Reference" spectrum measured in dust free Ar and Ar–NH_3 plasmas (blue) and typical spectrum in dusty Ar–CH_4 plasma (green)

Calculation of spectral density treating different sizes as distinct charged species in the multicomponent approach

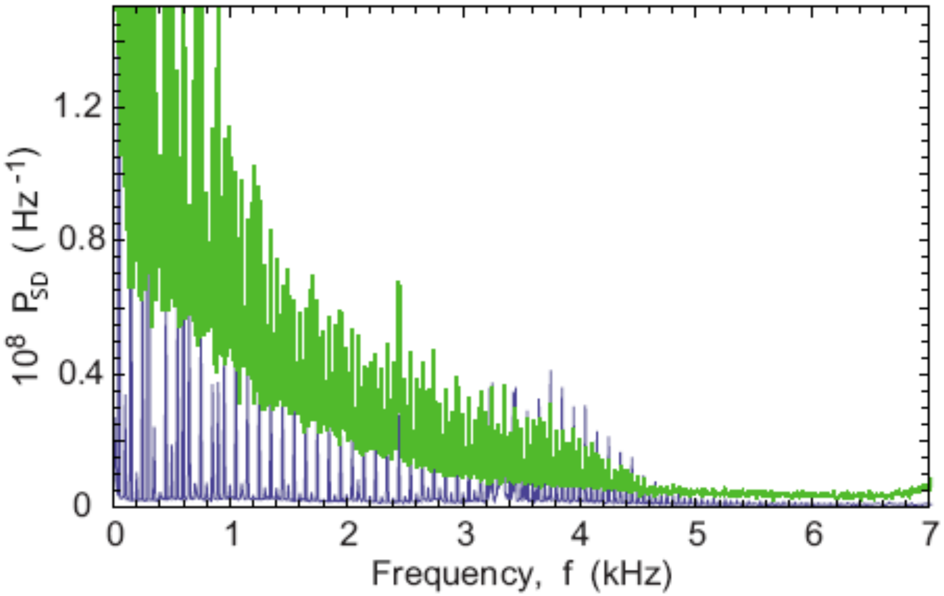

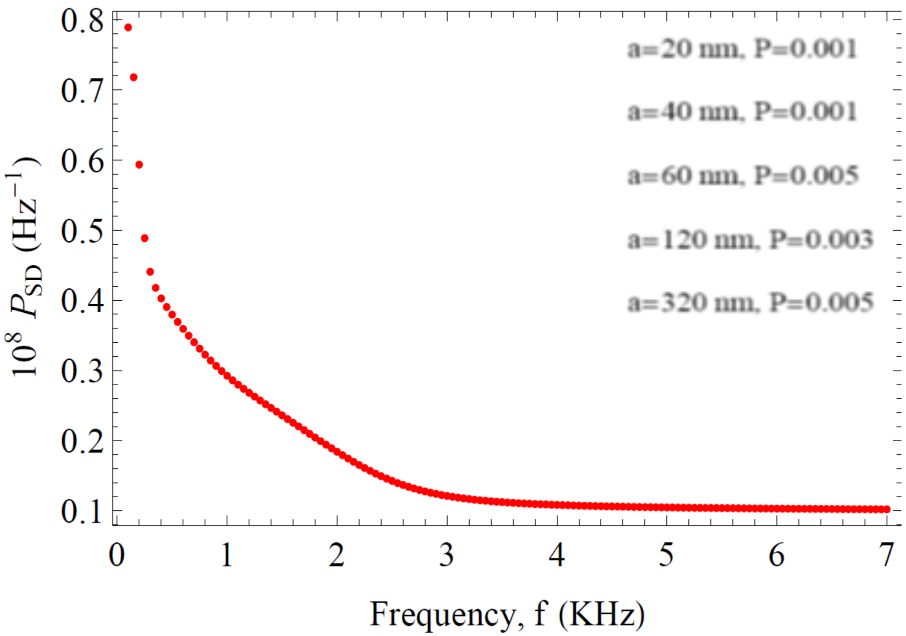

Ratynskaia S, De Angeli M, Lazzaro E, Marmolino C, de Angelis U, Castaldo C, Cremona A, La Guardia L, Gervasini G, Grosso G, PoP **17**, 043703 (2010)

The differential cross section for plasma scattering of radiation

$$\frac{d^2\sigma}{d\Omega d\omega_s} = \frac{3}{32\pi^2}\sigma_T\left[1+\cos^2\theta\right]S^e_{k,\omega}$$

$$\omega = \omega_s - \omega_i; \quad \vec{k} = \vec{k}_s - \vec{k}_i; \quad k = \left(k_s^2 + k_i^2 - 2k_s k_i \cos\theta\right)^{1/2}$$

$$\frac{v}{c} << 1; \quad k_s \cong k_i \cong \frac{\omega_i}{c} \rightarrow k \cong 2k_i \sin\frac{\theta}{2}$$

The spectral density of the electron density fluctuations

$$S^{e}_{k,\omega} = \left\langle \delta n^{e}_{k,\omega} \cdot \delta n^{e*}_{k,\omega} \right\rangle = S^{e(o)}_{k,\omega} \left(1 - 2\,\mathrm{Re}\left\{ \frac{\chi^{e*}_{k,\omega}}{\varepsilon_{k,\omega}} \right\} \right) + \frac{\left|\chi^{e}_{k,\omega}\right|^{2}}{\left|\varepsilon_{k,\omega}\right|^{2}} \left(S^{i(o)}_{k,\omega} + S^{e(o)}_{k,\omega} + Z_d^2 S^{d(o)}_{k,\omega} \right)$$

$$S^{\alpha(o)}_{k,\omega} = \left\langle \delta n^{\alpha(o)}_{k,\omega} \cdot \delta n^{\alpha(o)*}_{k,\omega} \right\rangle = 2\pi \int \Phi^{\alpha}(\vec{v}) \delta\left(\omega - \vec{k} \cdot \vec{v} \right) d\vec{v} = \sqrt{2\pi}\, \frac{n_\alpha}{k v_{T_\alpha}}\, e^{-\left(\frac{\omega}{\sqrt{2} k v_{T_\alpha}} \right)^2}$$

$$\frac{Z_d^2 S^{d(o)}_{k,\omega}}{S^{i(o)}_{k,\omega}} \approx P Z_d \left(\frac{m_d}{m_i} \right)^{1/2} e^{-\left(\frac{\omega}{\sqrt{2} k v_{T_d}} \right)^2} \approx 10^3$$

$$\left(\omega = \omega_s - \omega_i \simeq 0; P Z_d \approx 1; a = 10 nm \right)$$

Approach # 1:

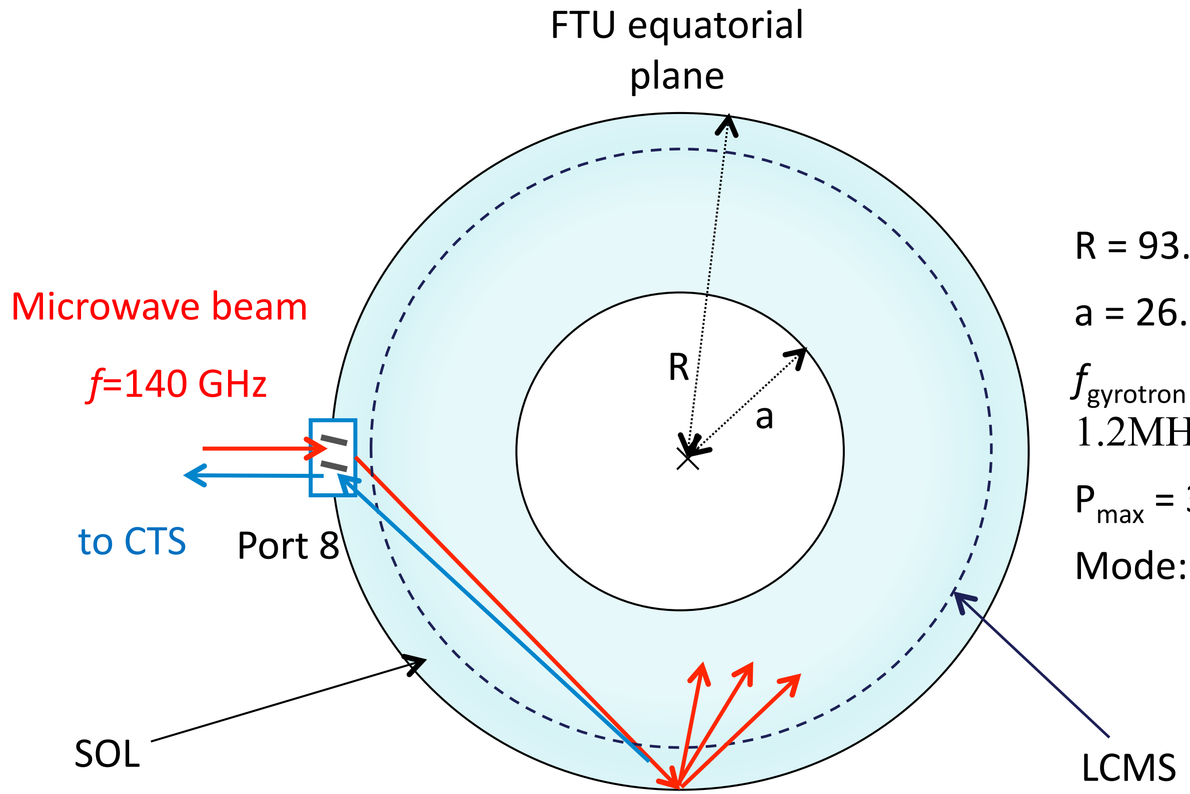

R = 93.5 cm

a = 26.9 cm

$f_{gyrotron}$ = 140GHz ± 1.2MHz

P_{max} = 300 kW

Mode: Gaussian

Approach # 2:

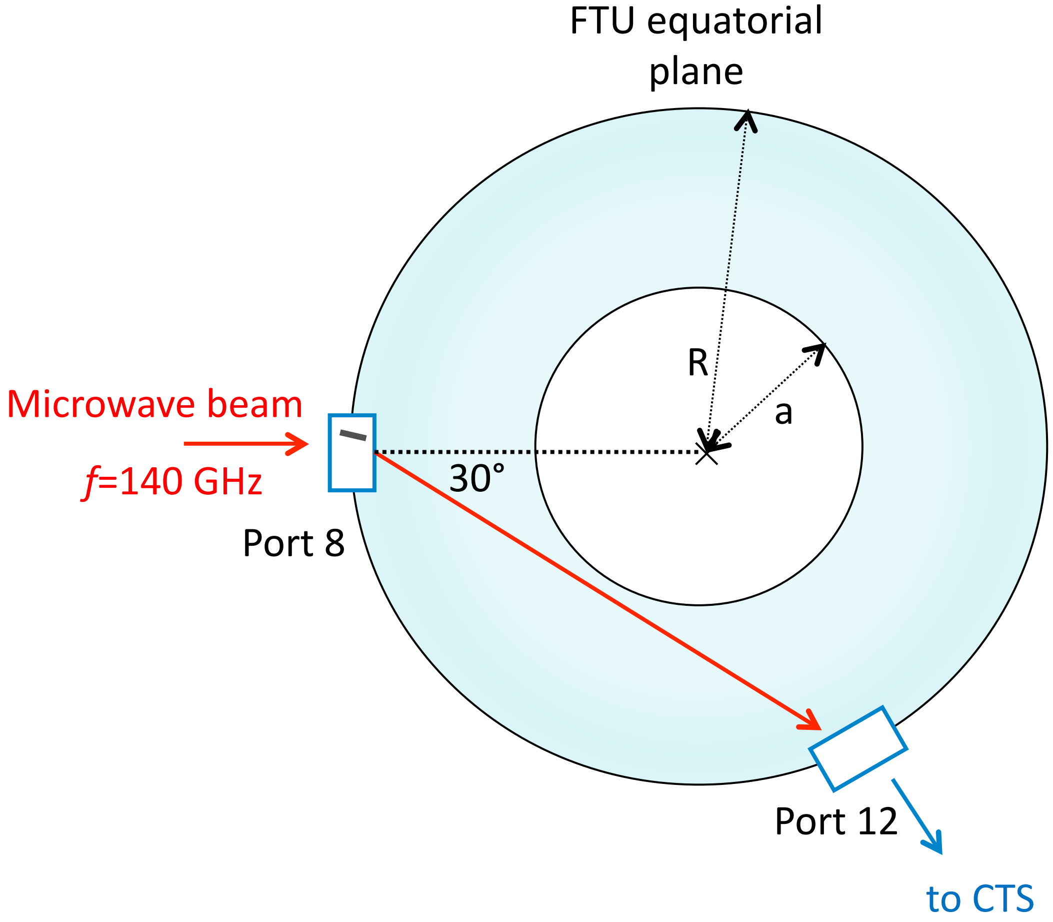

R = 93.5 cm

a = 26.9 cm

$f_{gyrotron}$ = 140GHz ± 1.2MHz

P_{max} = 300 kW

Mode: Gaussian

Conclusions

- How much submicron dust is present in tokamaks during operations?